Title

The Effect of the Kerguelen Plateau on the Ocean Circulation

Journal

Journal of Physical Oceanography, 46(11)

ISSN

0022-3670

Authors

Wang, Jinbo
Mazloff, Matthew R
Gille, Sarah T

Publication Date

2016

DOI

10.1175/jpo-d-15-0216.1

Peer reviewed

SPECIAL
DIMES
COLLECTION

The Effect of the Kerguelen Plateau on the Ocean Circulation

JINBO WANG,[a] MATTHEW R. MAZLOFF, AND SARAH T. GILLE

Scripps Institution of Oceanography, University of California, San Diego, La Jolla, California

(Manuscript received 6 November 2015, in final form 19 August 2016)

ABSTRACT

The Kerguelen Plateau is a major topographic feature in the Southern Ocean. Located in the Indian sector and spanning nearly 2000 km in the meridional direction from the polar to the subantarctic region, it deflects the eastward-flowing Antarctic Circumpolar Current and influences the physical circulation and biogeochemistry of the Southern Ocean. The Kerguelen Plateau is known to govern the local dynamics, but its impact on the large-scale ocean circulation has not been explored. By comparing global ocean numerical simulations with and without the Kerguelen Plateau, this study identifies two major Kerguelen Plateau effects: 1) The plateau supports a local pressure field that pushes the Antarctic Circumpolar Current northward. This process reduces the warm-water transport from the Indian to the Atlantic Ocean. 2) The plateau-generated pressure field shields the Weddell Gyre from the influence of the warmer subantarctic and subtropical waters. The first effect influences the strength of the Antarctic Circumpolar Current and the Agulhas leakage, both of which are important elements in the global thermohaline circulation. The second effect results in a zonally asymmetric response of the subpolar gyres to Southern Hemisphere wind forcing.

1. Introduction

Gill and Bryan (1971, p. 685) asked, ''What would happen to the world's ocean circulation if the Drake Passage were closed?'' By conducting a series of numerical simulations with differing bathymetries, they showed that closing Drake Passage (DP) not only led to the disappearance of the Antarctic Circumpolar Current (ACC) but also had a profound impact on the global-scale circulation and on intermediate water formation in the region. While the Drake Passage allows the ACC to exist, the Kerguelen Plateau (KP), one of the biggest ocean ridges in the Southern Ocean, alters and steers the ACC. The KP deflects the northern ACC front, that is, the Subantarctic Front (SAF), equatorward toward the energetic, warm, and saline Agulhas Return Current and adjacent subtropical front. The confluence of these currents leads to instabilities and the presence of high mesoscale eddy energy downstream of the plateau, which subsequently results in intense mixing and biological productivity (Gille 1997; Jayne and Marotzke 2002; Fu 2009; Lu and Speer 2010; Sallée et al. 2011; Waterman et al. 2013; Gille et al. 2014; Rosso et al. 2014). Even with these circulation patterns, it is unclear, however, whether there exists a Kerguelen Plateau effect as important as the Drake Passage effect with respect to the global ocean properties.

As a major bathymetric feature of the Southern Ocean, the KP is located in the southern Indian Ocean at about 75°E (Fig. 1). It extends more than 2200 km from 46° to 64°S in a tilted northwest–southeast direction and separates the Weddell–Enderby Basin to its west and the Australian–Antarctic Basin to its east. The Fawn Trough at about 56°S splits the plateau into two parts, the northern and southern Kerguelen Plateau. The southern KP was formed about 80–110 million years ago, while the northern KP was formed in the Cenozoic period (65 million years ago to present; Frey et al. 2000). In comparison, Drake Passage was formed about 17–50 million years ago (Livermore et al. 2005), and the opening of the Tasman Seaway is dated to 35.5–30 million years ago (Barker et al. 2007). The Kerguelen Islands and the Heard/McDonald Islands are located on the

[a] Current affiliation: Jet Propulsion Laboratory, California Institute of Technology, Pasadena, California.

Corresponding author address: Jinbo Wang, 4800 Oak Grove Dr., Pasadena, CA 91109.
E-mail: jinbow@alum.mit.edu

DOI: 10.1175/JPO-D-15-0216.1

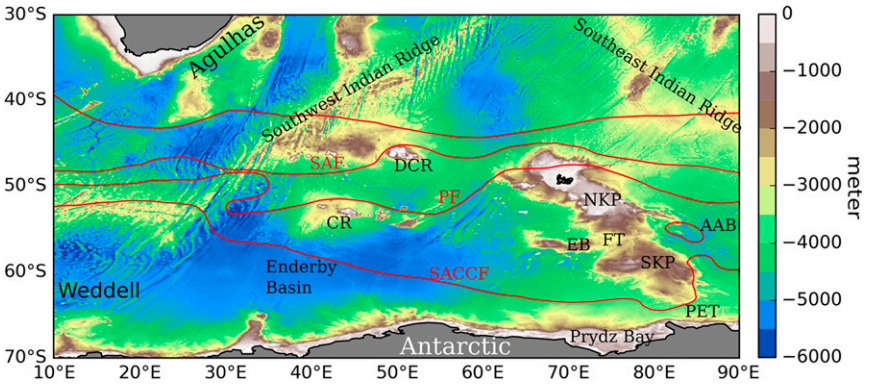

FIG. 1. The ocean bathymetry near the Kerguelen Plateau and the position of three ACC fronts. The ACC fronts identified by Orsi et al. (1995) are shown in red lines, that is, the SAF, PF, and SACCF. The abbreviations of topographic features are the Northern Kerguelen Plateau (NKP), Southern Kerguelen Plateau (SKP), Del Cano Rise (DCR), Conrad Rise (CR), Elan Bank (EB), Fawn Trough (FT), Australian–Antarctic Basin (AAB), and Princess Elizabeth Trough (PET).

northern Kerguelen Plateau, which is surrounded by the Del Cano Rise, the Crozet Plateau, and the Conrad Rise to its west and by the Kerguelen–Amsterdam Passage to its north. To the west of the Fawn Trough lies the Elan Bank with a sill depth shallower than 2000 m. The Princess Elizabeth Trough lies between the southern Kerguelen Plateau and the Antarctic coast. Prydz Bay, located at 75°E to the southwest of the Princess Elizabeth Trough, is a formation region of Antarctic Bottom Water (AABW; Meijers et al. 2010; Wong et al. 1998; Ohshima et al. 2013). The complex bathymetric configuration around the KP results in complicated bathymetry–flow interactions.

To understand bathymetry–flow interaction, it has been a common practice to conduct a sensitivity test by modifying ocean bathymetry in a model (e.g., Gill and Bryan 1971; Lee et al. 2002). Here, we follow the approach of Gill and Bryan (1971) on the effect of the Drake Passage and ask what would happen to the world's ocean if the Kerguelen Plateau were removed? The meridional meandering of the ACC would certainly be reduced due to the absence of blocking by the plateau, but would the rest of the ocean circulation also be affected?

In this paper, the effect of KP on the global ocean circulation is studied using a set of numerical global ocean simulations with and without the plateau. Based solely on the coarse-resolution simulation in this study, we show that KP has two important impacts on the global ocean circulation. First, the upstream pressure field supported by the plateau results in a reduction in the Agulhas leakage. Second, the pressure field diverts the SAF northward, generating a stagnant region upstream of the plateau and reducing the cross-frontal exchange between the subtropics and the Weddell Sea. The rest of the paper is organized as follows: The Kerguelen Plateau and the surrounding general ocean circulation are described in section 2. Section 3 discusses the numerical model setup. Results are presented in section 4. Discussion and conclusions are presented in section 5.

2. The effect of Kerguelen Plateau

a. Steering effect on the ACC

The KP lies at the same latitude as Drake Passage and strongly steers the eastward-flowing ACC (Gille 1994; Davis 2005; LaCasce and Isachsen 2010). The main transport of the ACC is carried by three fronts, the SAF, the Polar Front (PF), and the Southern ACC Front (SACCF), and these are packed within a 7° latitude span at 30°E. The SAF bends northward and flows through the Kerguelen–Amsterdam Passage. The SACCF is deflected southward through the Princess Elizabeth Trough (Fig. 1). The position of the PF is highly variable. Because of the blocking by the Kerguelen Plateau, the wedgelike envelope of the ACC between the SAF and the SACCF is widest at 75°E. The meridional shift of the mean ACC fronts form standing meanders strongly affecting the ACC momentum and tracer budgets.

Recent studies using high-quality synoptic hydrography and satellite data show inconsistent frontal positions (Fig. 1). For example, Dong et al. (2006) showed evidence that the surface expression of the PF goes through the Kerguelen–Amsterdam passage, while Sparrow et al. (1996) noted that the PF is composed of a single frontal jet at 30°E but splits into two branches as the surface and subsurface temperature, and salinity properties are no longer consistent. Sparrow et al. (1996) suggested that the surface PF goes through the Fawn Trough, while Park et al. (2009) identified the current in Fawn Trough as the SACCF. The discrepancies in the

literature are partially due to inconsistencies in the definition of the front, as dynamical fields such as sea surface height (SSH) and tracer fields show different frontal positions, but they are also due to the highly fluctuating nature of the fronts in this bathymetrically complex region.

Previous studies indicate that the existence of the Kerguelen Plateau leads to a complex regional ACC structure (e.g., Sparrow et al. 1996; Park et al. 2009; Rosso et al. 2015), but its impacts on the basin- and global-scale ocean circulation remain unclear.

b. *Influence on ACC dynamics*

The wind-driven acceleration of the ACC can only be balanced by bottom form stress because bottom friction and lateral Reynolds stress are too weak to balance the surface wind stress without generating unrealistically strong flow (Toggweiler and Samuels 1995; Marshall and Radko 2003; Munk and Palmen 1951; Gille 1997). The form stress by four major ridges, the Scotia Arc, the Kerguelen Plateau, the Macquarie Ridge, the South Pacific Ridge, and South America is suggested to balance the zonal wind stress in the Drake Passage latitudes (Masich et al. 2015). Eddy interfacial form stress transfers surface momentum downward to depths where bottom form stress can have an impact. This balance is related to the horizontal eddy buoyancy flux through the thermal wind relation. The eddy effect slumps the tilted isopycnals, counteracts the continual acceleration of the zonal flow by the wind, and sets the vertical structure of the ACC (Johnson and Bryden 1989).

The local enhancement of eddy kinetic energy by topography has been emphasized to be crucial in setting ACC properties. Bathymetric steering can raise or slump ACC fronts to alter the flow instability properties and subsequently eddy generation and destruction. Enhanced eddy kinetic energy in the lee of topographic obstacles has long been observed (Gille 1997; Lu and Speer 2010; Sallée et al. 2011; Thompson and Sallée 2012) and theorized (MacCready and Rhines 2001). The enhanced eddy activities result in hot spots of mass, momentum, potential vorticity, heat, and tracer transport. Williams et al. (2007) drew an analogy between the storm tracks in the atmosphere and the ACC, noting that topographic effects lead to along-stream variations in eddy potential vorticity fluxes, which can decelerate or accelerate the mean flow. Based on a similar view, Thompson and Naveira Garabato (2014) put forward a theory for the equilibration of the ACC in which the structure of the standing meanders, rather than intensity of transient baroclinic instabilities, governs the ACC response to wind forcing and changes.

These topographically enhanced standing meanders result from arrested Rossby waves and enable rapid downward moment transfer and bottom stress. The study by Thompson and Naveira Garabato (2014) points to the necessity of understanding the ACC from a localized view, recognizing zonal variations, rather than from a zonally averaged framework. The Kerguelen Plateau has a clear impact on localized standing and transient eddies, which in turn influence the entire ocean ACC properties.

Even though a growing body of evidence has demonstrated the importance of topographic control on ACC dynamics and Southern Ocean circulation, many questions still remain regarding the specific role of the Kerguelen Plateau. Here, we use a simplified numerical model to explicitly test the response of the Southern Ocean and the World Ocean to the Kerguelen Plateau.

3. Methodology

The complex nature of ocean dynamics makes direct evaluation of the large-scale effect of a specific regional seamount difficult. Here, we evaluate the effect of the KP on the large-scale ocean circulation by comparing simulations with and without the KP. The two simulations are carried out using two nearly identical configurations of the MITgcm (Marshall et al. 1997) that differ only in the bathymetry used for the KP region. The ETOPO5 5-min world bathymetry from 80°S to 80°N without the Arctic Ocean is binned to 1° × 1° resolution for the control run (CTRL). The perturbed case (noKP) has the same bathymetry as CTRL but with a flattened KP. To flatten KP, we set the ocean floor to 4700 m for all model grids within the domain (53°–35°S, 60°–87°E), then apply 5° × 5° two-dimensional Gaussian smoothing only near the KP to remove the induced, steep topographic slope.

Figure 2 shows the bathymetry of CTRL and noKP. We do not claim that the noKP bathymetry corresponds to a specific geological period. The altered seafloor is intended to help us gain physical understanding of the influence of KP on the ocean circulation.

The two simulations have the same surface forcing. The wind stress is based on Trenberth et al. (1989) climatology. The model is initialized with Levitus climatology (Levitus and Boyer 1994). The SST and sea surface salinity (SSS) are relaxed to the seasonal Levitus climatology to provide the surface forcing. The relaxation time scale is 2 months for temperature and 6 months for salinity.

We spin up the ocean by progressively increasing resolution for both CTRL and noKP cases. The model is first run for 1000 yr with 4° × 4° resolution in the horizontal and 15 levels in the vertical. The run continues

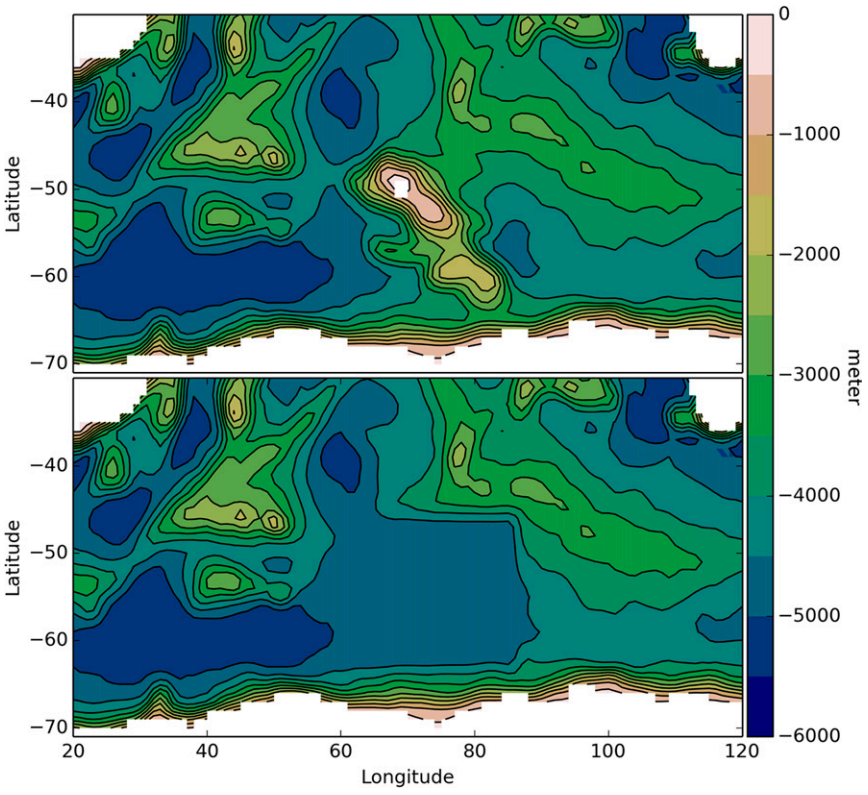

FIG. 2. The south Indian Ocean bathymetry used in (top) CTRL and (bottom) noKP.

with a 2° × 2° resolution for another 200 yr, followed by a 1° × 1° resolution with 25 vertical levels for another 1020 yr. The last 20 yr are used in the following analyses. In addition, we investigate the adjustment problem by adding back the Kerguelen Plateau to the noKP case starting from the end of the 1020 yr 1° × 1° simulation and running for another 20 yr. The horizontal viscosities are 5×10^5, 2×10^5, and $5 \times 10^3\,m^2\,s^{-1}$ for the 4° × 4°, 2° × 2°, and 1° × 1° simulations, respectively. The model employs the K-profile parameterization (KPP) for vertical mixing (Large et al. 1994) and fixed Gent–McWilliams (GM)/Redi eddy parameterization (Redi 1982; Gent and McWilliams 1990) for isopycnal eddy mixing. In the 1° × 1° run, the constant GM background diffusivity is $1 \times 10^3\,m^2\,s^{-1}$. A Laplacian diffusivity of $2 \times 10^3\,m^2\,s^{-1}$ is also used. The vertical Laplacian diffusivity ($1 \times 10^{-4}\,m^2\,s^{-1}$) and viscosity ($1 \times 10^{-3}\,m^2\,s^{-1}$) are fixed for the three different-resolution simulations. The model is in an equilibrated state in terms of kinetic energy but still drifts in temperature and salinity fields. However, these drifts (10^{-5} °C yr^{-1} for temperature and 10^{-7} psu yr^{-1} for salinity) are very slow compared to the changes due to the KP, which are $O(10^{-1})$ °C for temperature and $O(10^{-2})$ psu for salinity.

In the CTRL run, the zonal transport across the Drake Passage is 93.1 Sv (1 Sv ≡ $10^6\,m^3\,s^{-1}$), which is smaller than the observed 137 Sv (Cunningham et al. 2003). The Agulhas Current across 32°S is −64 Sv, comparable to the observed value of −70 Sv in Bryden et al. (2005). The Agulhas leakage is −32.3 Sv; much larger than the observed −15 Sv (Richardson 2007), but comparable to −32 Sv in a ½°-resolution model (van Sebille et al. 2009) and −43 Sv in a typical 1° CCSM4 simulation (Weijer et al. 2012). We do not aim to have the coarse-resolution simulation produce realistic values for the transport but instead focus on the changes brought by the change in KP topography.

4. Results

Differences exist both locally in the Southern Ocean and in the global ocean between the CTRL and noKP. In this section, we first discuss the KP effect on the Southern Ocean circulation and then we examine the effect on global thermohaline circulation.

a. Effect on the Southern Ocean circulation

Without the steering by the KP, the ACC becomes more zonal in the Indian sector. The shift of the ACC

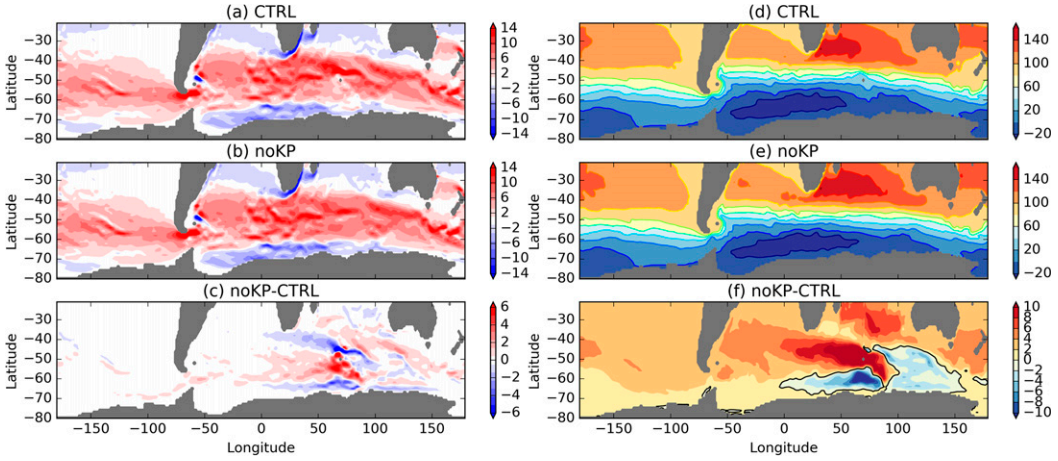

FIG. 3. (left) The vertically integrated zonal transport per grid box defined as $U = \Delta y \int_{-H}^{\eta} u\, dz$ in (a) CTRL, (b) noKP, and (c) their difference noKP − CTRL, where Δy is the meridional length of the model grid. (right) The barotropic streamfunction defined as $\Psi = \sum_y U$, with $\Psi = 0$ along the Antarctic continent in (d) CTRL, (e) noKP, and (f) their difference noKP − CTRL. All panels have units of Sv.

and the consequent influence on the circulation are clearly shown in zonal transport and streamfunction (Fig. 3). Here, the barotropic streamfunction is defined as $\Psi = \sum_y U$, where $U = \Delta y \int_{-H}^{\eta} u\, dz$ (Δy is the meridional length of the model grid) is the vertically integrated zonal transport per grid box, η is the surface height, $-H$ is the depth of the ocean bottom, and u is the zonal velocity. The boundary condition $\Psi = 0$ is given along the Antarctic boundary. Upon reaching the KP, the ACC fronts diverge (Fig. 3d). A significant portion of the transport is carried by the SAF around the northern tip of the northern Kerguelen Plateau, where the SAF intensifies and narrows. Without the KP, the streamfunction becomes more zonal (Fig. 3e), meaning that streamfunction contours that diverge in CTRL now remain parallel toward the KP longitude. This leaves a north–south dipole in the streamfunction difference field (Fig. 3f). The dipole is anticyclonic to the north and cyclonic to the south. This also means that the Weddell Gyre expands northward and the Indian Subtropical Gyre expands southward. The expansion of the two gyres significantly impacts the global thermohaline circulation as described in the next section.

The adjustment of the pressure field also leads to downstream differences in the zonal transport (Figs. 3a,b,c). Although broader and more laminar in this coarsely resolved model than observed in the real ocean, the ACC still shows segmented zonal jets induced by irregular bottom topography. The velocity fields in the two cases appear to agree well at the large scale (Figs. 3a,b) but differ significantly in the proximity of the KP (Fig. 3c). Without the KP, the zonal transport upstream of the KP shows a clear, positive change at the KP latitude sandwiched between two strips of negative change (Fig. 3c), meaning that the ACC is stronger at the KP latitude, the Agulhas Return Current (ARC) is weaker, and the westward boundary current along the Antarctic continent is stronger. Velocity changes are noticeable in Southern Ocean regions outside the Indian sector as well. One significant region is Drake Passage, where, in the noKP case, the zonal velocity is stronger and the ACC transport through the DP is 96.5 Sv, greater by about 3.5% (Fig. 4b). This change exceeds the interannual variability of the through DP transport and is statistically significant.

The changes in the Southern Ocean circulation are to a large extent vertically coherent. Figure 4 shows the latitude–depth section along 50°E of the zonal velocity difference between two cases (noKP − CTRL). A zonal average of 40°–50°E gives the same structure. The differences in the zonal velocity are surface intensified but extend deep, especially in the high-latitude regions where stratification is weak.

b. *Influence on form stress*

Both in this study and in previous studies based on scaling (Johnson and Bryden 1989) and numerical simulations (Killworth and Nanneh 1994; Gille 1997; Ivchenko et al. 1996; Stevens and Ivchenko 1997), the domain-integrated momentum balance in the Southern Ocean is between the momentum input by the surface wind and the momentum sink by the bottom form stress imposed by the pressure difference across submarine ridges.

Since the advection of momentum and the Coriolis terms do not contribute to the total balance, and the

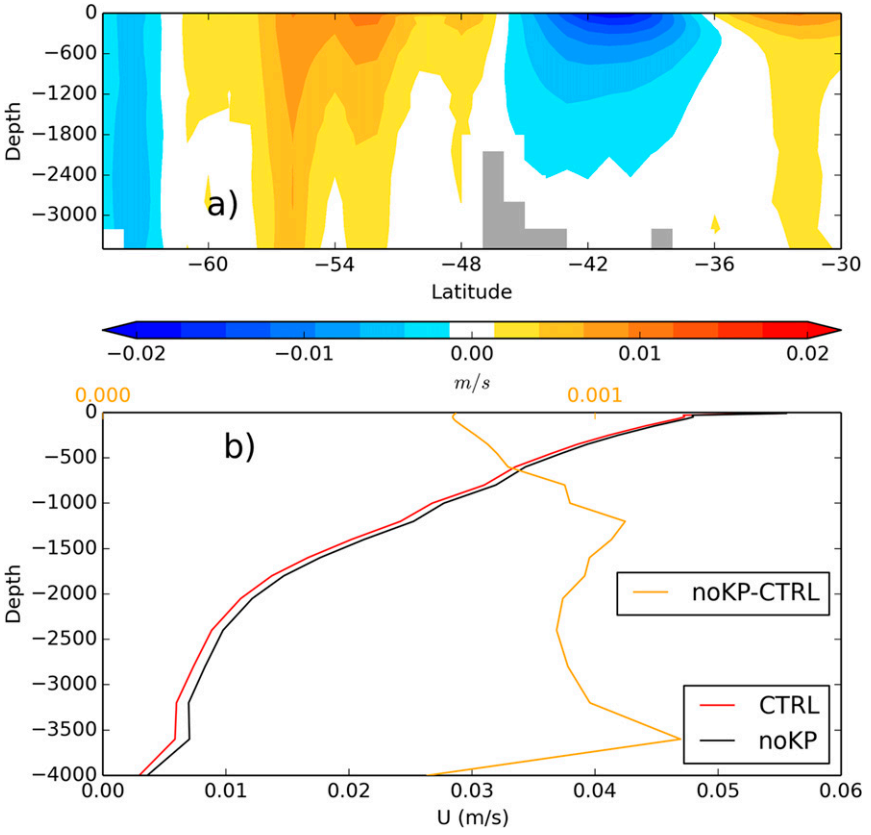

FIG. 4. (a) The depth–latitude section of the zonal velocity difference (noKP − CTRL) along 50°E. (b) The vertical profile of the mean zonal velocity at the entrance of the DP at 67°W.

other terms are small, we focus our analysis on the differences in bottom form stress between the CTRL and noKP cases.

The vertically and zonally integrated zonal momentum balance is approximately

$$0 \approx \oint\int_{-H}^{\eta} -\frac{1}{\rho_0}\frac{\partial \overline{p}}{\partial x}\,dz\,dx + \oint\frac{\tau^x}{\rho_0}, \tag{1}$$

where the overbar represents the time mean, H is the ocean depth, η is the sea surface height, ρ_0 is the reference density, $\overline{p}$ is the mean hydrostatic pressure, τ^x is the zonal wind stress, and $\oint$ is the zonal integration.

The integrated zonal momentum input by surface wind between 80° and 30°S is 8.0×10^{12} N in both the CTRL and noKP cases. The bottom form stress integrated over the same domain is 7.8×10^{12} N in CTRL and 7.9×10^{12} N in noKP, accounting for more than 97% of the total momentum input. The form stress increase in noKP is due to the decrease in bottom friction because of the flattening of the KP.

There are several ways of calculating the bottom form stress. After neglecting the contribution of atmospheric loading, which is usually negligible, the left-hand side of (2) consists of two components:

$$\oint\int_{-H}^{\eta} -\frac{1}{\rho_0}\frac{\partial \overline{p}}{\partial x}\,dz\,dx = -\oint_x \frac{\partial}{\partial x}\int_{-H}^{0} \overline{p}\,dz\,dx + \oint_x \overline{p_b}\frac{\partial H}{\partial x}\,dx, \tag{2}$$

where $\overline{p}_b$ is the bottom pressure. The first term on the right-hand side represents the net stress due to the pressure gradient across landmasses. The second term represents the bottom form stress. Here, we adopt the algorithm of Masich et al. (2015) treating both the landmasses and submerged seamounts as ''ridges'' and directly calculating the left-hand side without distinguishing the two components. The pressure gradient at a discretized model grid point (x, y, z) is calculated as

$$\frac{\partial \overline{p}}{\partial x}(x,y,z) = \frac{\Delta \overline{p_b}}{\Delta x} = \frac{\overline{p_b}(y,z\,|\,x_E) - \overline{p_b}(y,z\,|\,x_W)}{x_E - x_W}, \tag{3}$$

where x_E and x_W are the eastern and western sides of an ocean ridge that encloses the model grid point (x, y, z); $\overline{p_b}(y, z\,|\,x_E)$ and $\overline{p_b}(y, z\,|\,x_W)$ are the bottom pressure at

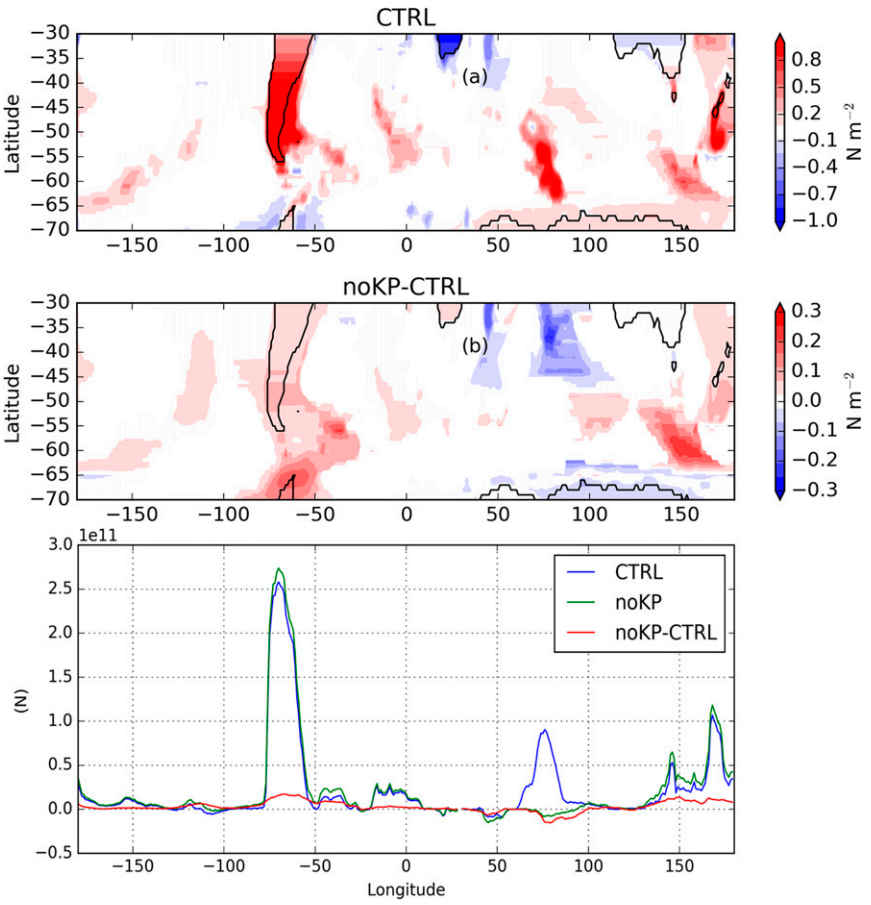

FIG. 5. (a): The bottom form stress F in CTRL (N m^{-2}). Positive means eastward momentum transfer from the ocean to the solid earth. (b) The form stress difference between noKP and CTRL (noKP − CTRL). Positive means more eastward momentum is transferred from the ocean to the solid earth in noKP. Note that the Kerguelen Plateau is masked out in (b). (c) The meridionally integrated (35°–65°S) bottom form stress per grid box denoted by $\Delta x \int_y F\, dy$, where Δx is the length of the model grid. The deep ocean below 4200 m is masked out.

the two ridge walls. The east–west pressure difference across a ridge is distributed uniformly inside the ridge. We choose this uniform pressure distribution within land for visualization purposes (see Fig. 2 of Masich et al. 2015). The values can be regarded as momentum transfer of ocean currents *into* the solid earth. This quantity is visually patchy for each level, but its full-depth vertical integration yields a smoother field. The vertical integration of (3) is referred to as total bottom form stress and shown in Fig. 5. As shown by Masich et al. (2015), this method reduces the numerical noise brought by calculating the gradient of H. The budget in (1) can be accurately closed.

The total bottom form stress is concentrated over several major topographic features, including the KP, the Macquarie Ridge region, the East Pacific Rise, the Drake Passage, the South American continent, and the Mid-Atlantic Ridge. Table 1 lists the partitioning of the bottom form stress in each of the major regions. Based on the integration between 65° and 35°S, the KP region explains about 16% of the total bottom form stress. About 23% resides around the Macquarie Ridge region, and more than half is associated with the DP and South American continent. The Pacific Rise and Mid-Atlantic Ridge account for about 3%–5%. The bottom form stress supported by the KP in CTRL is redistributed about equally between the Macquarie Ridge region and the DP/South American region in noKP. The partitioning of the form stress is sensitive to the meridional extent of the integration. For example, moving the northern boundary from 35° to 50°S increases the KP region to 28% and the MR region to 27% and decreases the DP/South American region to 30% in CTRL. But the partitioning of the missing KP form stress between the Macquarie Ridge and DP/South America is not sensitive to the integration domain.

TABLE 1. The percentage of form stress explained by the KP region (50°, 120°E), Macquiere Ridge (MR) region (120°E, 20°W), South Pacific (20°, 90°W), DP region (90°, 30°W), and South Atlantic/Indian (50°E, 30°W). The regional partitioning is based on the integration between 65° and 35°S. Changing the northern boundary to 50°S increases the percentage of the KP and MR to 28% and 27%, respectively, and reduces the percentage of the DP to 30% in CTRL.

Case/region	KP	MR	Pacific	DP	Atlantic/Indian
CTRL	16	23	3	53	5
noKP	1	30	3	60	6

The ACC transport through DP is not directly linked to how the form stress is distributed. We conduct an additional experiment to study the transient behavior of the bottom form stress by adding the KP back to the noKP case. After adding back the KP bathymetry, the bottom form stress is quickly redistributed in less than 50 days followed by a clear seasonal cycle, while the ACC transport through DP changes slowly at a rate of about 0.5 Sv decade^{-1} (figure not shown). The quick response is associated with fast barotropic response (Straub 1993) and is demonstrated clearly in the idealized channel model by Ward and Hogg (2011). The ACC transport is linked to the baroclinic structure and is influenced by meridional buoyancy transport, including eddy fluxes (Allison et al. 2011), which are parameterized by GM in our model.

In summary, the KP accounts for more than 16% of the removal of the zonal momentum injected by wind, but the same momentum balance can be achieved without the existence of the KP. Without KP, the KP bottom form stress is about equally redistributed to the Macquarie Ridge and the DP/South American continent. The total bottom form stress is barely affected. The bottom form stress adjusts to the topographic change through a fast barotropic adjustment in less than 50 days, but the ACC transport responds to the Southern Ocean thermohaline adjustment, which takes several decades in this diffusive simulation.

c. *Effect on global thermohaline circulation*

Because of the differences in the circulation, there exist differences in the global ocean thermohaline structure between the CTRL and noKP.

In the Southern Ocean, without the KP, the upper ocean (0–1000 m) to the west of KP becomes warmer and saltier (Figs. 6a,c). The warm, saline sea surface anomaly extends upstream to the Atlantic Ocean, reaching as far as the Brazil–Malvinas Confluence. The upper southeast Indian Ocean east of KP becomes colder and fresher. The fresh anomaly influences the north Indian Ocean and also propagates into the South Atlantic through the Agulhas leakage. The surface restoration is faster for the temperature (2 months) than for the salinity (6 months). As a result, the cold anomaly initiated near the KP is more confined to the source region than the fresh anomaly. The upper Pacific Ocean becomes warmer and saltier except in the Amundsen Sea, where cold and fresh anomalies are present.

The differences in the regional circulation in the upper ocean (Fig. 3) explain the thermohaline differences; a weaker and southward-shifted subtropical front and Agulhas return current decrease the heat and salt transport to the northeast of the KP (Fig. 6) and increases heat and salt transport to the southwest. The reduction of the

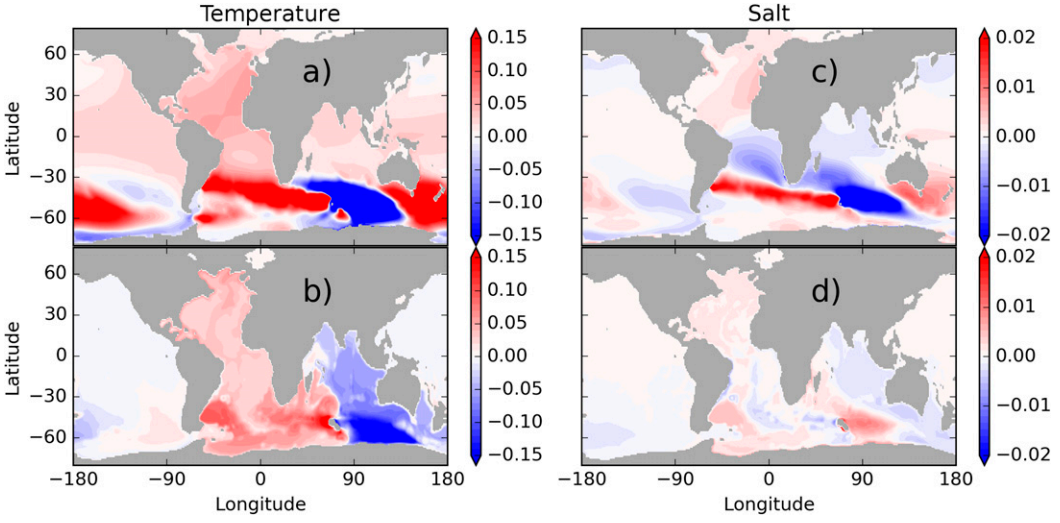

FIG. 6. The (a),(b) temperature (°C) and (c),(d) salinity (psu) differences between CTRL and noKP (noKP − CTRL) for the (top) upper (0–1000 m) and (bottom) deep ocean average below 1000 m.

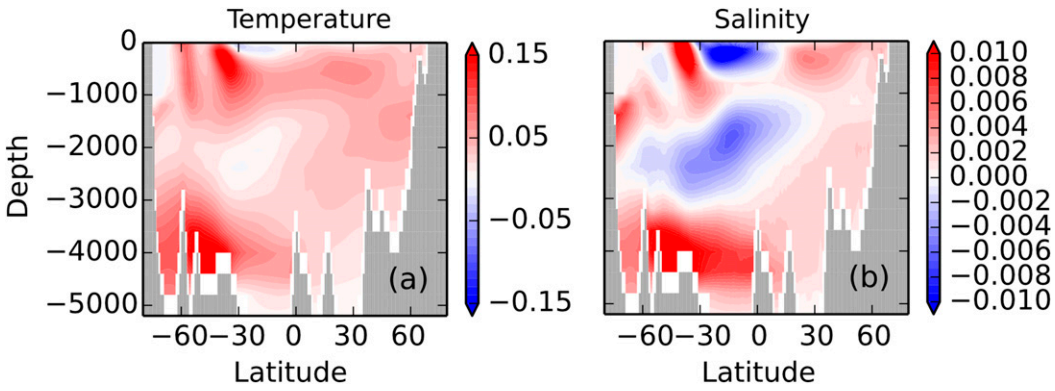

FIG. 7. The depth–latitude sections of (a) temperature (°C) and (b) salinity (psu) differences between CTRL and noKP (noKP − CTRL) along 25°W in the Atlantic.

southward deflection of the flow passing the northern edge of the KP at 80°E and the excess northward transport east of KP (Fig. 4d) further introduce cold and fresh anomalies downstream of the KP (Figs. 6a,c).

For the global ocean, in the noKP case, the North Atlantic, far from the KP, becomes warmer and saltier throughout the water column. These changes may have an impact on abyssal ocean circulation and global climate due to the crucial role of the North Atlantic in the climate system.

A depth–latitude section of the anomaly field shows that the warm anomaly appears both in the upper cell of the meridional overturning circulation near 1000 m and in the lower cell, that is, in the deep Weddell Gyre near 4000 m and near 2500 m in the North Atlantic (Fig. 7).

These temperature and salinity changes may be induced by the changes in the Atlantic meridional overturning circulation (AMOC; Fig. 8). The CTRL run reproduces an AMOC with a reasonable depth and strength (Fig. 8a). We take the vertical derivative of the AMOC streamfunction to get the meridional volume transport per meter (Sverdrups per meter), which is equivalent to the zonal integration of meridional velocity. Figure 8b shows the difference between CTRL and noKP. Without KP, the northward transport in the upper cell becomes shallower, that is, the flow in the upper 500 m becomes faster and the flow between 500 and 1000 m becomes slower. The southward flow around 2000 m carrying the North Atlantic Deep Water (NADW) has a positive anomaly, meaning that the transport becomes weaker. Similarly, the deep northward flow carrying AABW has negative anomaly, meaning the deep export of AABW also becomes weaker. In our proposed mechanism, all these changes in the AMOC begin with the changes in the Indian–Atlantic exchanges through the passage of the Agulhas leakage due to the remote influence by the KP.

After considering all the results of the coarse-resolution model, we propose the following hypothesis of the KP effect. Without the KP, the ACC in the Indian sector becomes more zonal and shifts southward (Figs. 3d,e). This southward shift of ACC fronts leads to the southward shift of the subtropical front and Agulhas Return Current, which results in more transport of Indian water to the Atlantic through Agulhas leakage (Figs. 3c, 4a). The increased Agulhas leakage induces a warm anomaly over the whole upper Atlantic Ocean (Fig. 6a). The induced warm anomaly over the North Atlantic can further reduce the production of the NADW and causes a slowdown of the southward transport of NADW around 2000 m deep (Fig. 8b). The northward veering of the northern ACC fronts can shield Weddell from the influence of the Indian Ocean. Without the KP, the deep Weddell becomes warmer and salter due to the influence of the Indian water (Figs. 6b,d, 7), resulting in less AABW outflow (Fig. 8b). Because of the flattening of the KP, the Atlantic meridional heat transport increases by 3.5% (figure not shown). A caveat is that the hypothesis is based on the coarse-resolution simulation. The ''gate keeper'' effect of the subtropical front and South Atlantic Current at the Agulhas leakage may not be valid in high-resolution simulations or reality (Loveday et al. 2014; Durgadoo et al. 2013). Our ocean-only simulation does not fully evaluate the significance of this effect to the climate system, but this could be tested in a coupled model.

5. Discussion and conclusions

The KP is located in a sensitive region where the topographically induced regional circulation forces an upstream change in the Subtropical Front, Agulhas Return Current, and further, the Agulhas leakage to the south of

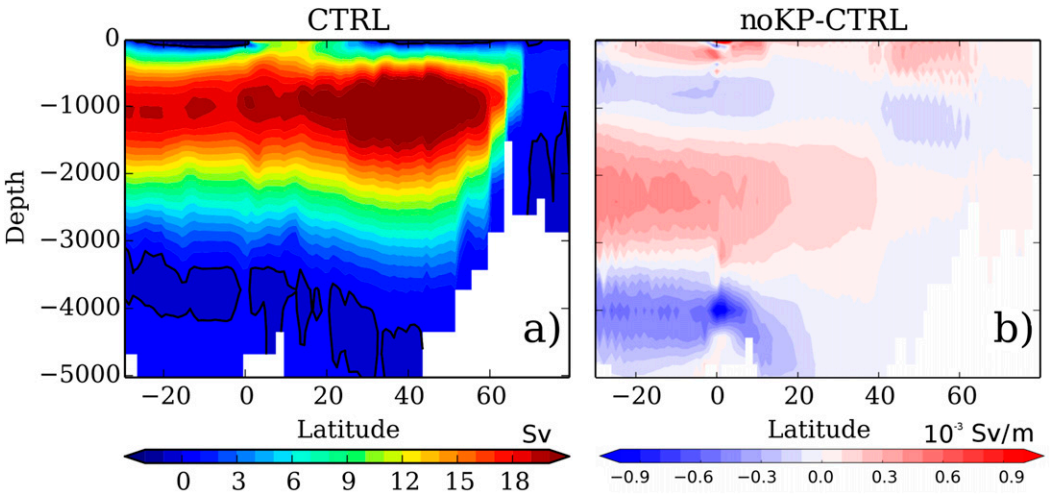

FIG. 8. (a) The Atlantic meridional overturning circulation in CTRL (Sv) and (b) the vertical derivative of the difference between the AMOCs in two simulations (noKP − CTRL) (10^{-3} Sv m^{-1}). It is equivalent to the zonal integration of meridional velocity.

the African continent, which is the prime exchange pathway between the Indian and Atlantic Oceans.

The KP accounts for about 16% of the total bottom form stress that balances the wind stress, but the KP is not critical for the balance. Without the KP, the 16% form stress imposed by KP is approximately equally redistributed to the Macquarie Ridge region (Southeast Indian Ridge, Macquarie Ridge, and Campbell Plateau) and the DP/South American continent. The mean zonally and vertically integrated momentum balance is still between wind stress and bottom form stress.

The ACC transport through the DP is not directly linked to the way the bottom form stress is distributed but rather is related to the bathymetric effect on the Southern Ocean thermohaline structure. The adjustment of the bottom form stress is associated with fast barotropic processes on time scales less than 50 days, but the ACC transport adjustment to the bathymetric change near KP takes several decades.

Without the KP, the ocean surface is warmer within the ACC, except in the region downstream of KP in the southeast Indian Ocean. The ocean surface is warmer over the North Atlantic, despite the quick (2 months) SST restoration. Moreover, almost the whole North Atlantic is warmer without the KP. The regionally modified heat and salinity budget has an up-scaling effect and influences the large-scale ocean circulation and the meridional ocean heat transport. The northward meridional heat transport is about 3.5% larger without the KP.

These modeled differences in the hypothetical ocean could potentially influence other components of Earth's climate system, if coupling among them were allowed. For example, the presence of KP deflects SACCF southward, which may result in a direct modulation of ocean–cryosphere interaction near Prydz Bay and the associated bottom water formation. However, the most important point of this paper is not to demonstrate what could happen if the KP were removed but to demonstrate the effect of the KP on the existing environment.

The limitations of this study come from the model configuration. The resolution is coarse, as in most coupled climate models, so that the eddy effects are parameterized as having fluxes proportional to local isopycnal slope. Local transports from eddy processes are thus represented, though the magnitudes of the fluxes have heightened uncertainty with respect to eddy-resolving runs. While the local eddy flux response to the removal of Kerguelen Plateau is represented, nonlocal eddy fluxes as Southern Ocean eddies can live for months and propagate far from formation locations (Hallberg and Gnanadesikan 2006). Nonlocal eddy transport is especially relevant to Agulhas leakage, which is through eddies but only represented by direct transport in the coarse-resolution model. Resolving eddies could make the flow less sensitive to topographic features, and eddies may make the KP solution more like the noKP solution with regards to the effect on the ACC circulation. The KP is found to account for a large portion of the BFS, however, making it doubtful that the influence of the pressure field setup by KP could be fully compensated by eddy dynamics. The veering response of the ACC to KP is apparent in observations. The parameterization of eddies results in an increased uncertainty with regards to quantifying the KP effect, but the enhanced asymmetry in hydrographic properties between the Atlantic and Indian Oceans due to the influence of KP on the pressure field is a robust

feature. There is no coupling with the atmosphere or cryosphere. Although the results of this study are physically sound, further research with a more realistic climate model configuration would be worth pursuing.

Acknowledgments. Wang, Mazloff, and Gille are supported by NSF OCE-1234473 and PLR-1425989. We thank Jessica Masich, Lynne Talley, Andy Hogg, Paola Cessi, Wei Liu, and two anonymous reviewers for their comments.

REFERENCES

Allison, L. C., H. L. Johnson, and D. P. Marshall, 2011: Spin-up and adjustment of the Antarctic Circumpolar Current and global pycnocline. *J. Mar. Res.*, **69**, 167–189, doi:10.1357/002224011798765330.

Barker, P., B. Diekmann, and C. Escutia, 2007: Onset of Cenozoic Antarctic glaciation. *Deep-Sea Res.*, **54**, 2293–2307, doi:10.1016/j.dsr2.2007.07.027.

Bryden, H. L., L. M. Beal, and L. M. Duncan, 2005: Structure and transport of the Agulhas Current and TTS temporal variability. *J. Oceanogr.*, **61**, 479–492, doi:10.1007/s10872-005-0057-8.

Cunningham, S., S. Alderson, B. King, and M. Brandon, 2003: Transport and variability of the Antarctic Circumpolar Current in Drake Passage. *J. Geophys. Res.*, **108**, 8084, doi:10.1029/2001JC001147.

Davis, R. E., 2005: Intermediate-depth circulation of the Indian and South Pacific Oceans measured by autonomous floats. *J. Phys. Oceanogr.*, **35**, 683–707, doi:10.1175/JPO2702.1.

Dong, S., J. Sprintall, and S. T. Gille, 2006: Location of the Antarctic polar front from AMSR-E satellite sea surface temperature measurements. *J. Phys. Oceanogr.*, **36**, 2075–2089, doi:10.1175/JPO2973.1.

Durgadoo, J. V., B. R. Loveday, C. J. C. Reason, P. Penven, and A. Biastoch, 2013: Agulhas leakage predominantly responds to the Southern Hemisphere westerlies. *J. Phys. Oceanogr.*, **43**, 2113–2131, doi:10.1175/JPO-D-13-047.1.

Frey, F., and Coauthors, 2000: Origin and evolution of a submarine large igneous province: The Kerguelen Plateau and Broken Ridge, southern Indian Ocean. *Earth Planet. Sci. Lett.*, **176**, 73–89, doi:10.1016/S0012-821X(99)00315-5.

Fu, L.-L., 2009: Pattern and velocity of propagation of the global ocean eddy variability. *J. Geophys. Res.*, **114**, C11017, doi:10.1029/2009JC005349.

Gent, P. R., and J. C. McWilliams, 1990: Isopycnal mixing in ocean circulation models. *J. Phys. Oceanogr.*, **20**, 150–155, doi:10.1175/1520-0485(1990)020<0150:IMIOCM>2.0.CO;2.

Gill, A., and K. Bryan, 1971: Effects of geometry on the circulation of a three-dimensional Southern-Hemisphere ocean model. *Deep-Sea Res. Oceanogr. Abstr.*, **18**, 685–721, doi:10.1016/0011-7471(71)90086-6.

Gille, S. T., 1994: Mean sea surface height of the Antarctic Circumpolar Current from Geosat data: Method and application. *J. Geophys. Res.*, **99**, 18 255–18 273, doi:10.1029/94JC01172.

——, 1997: The Southern Ocean momentum balance: Evidence for topographic effects from numerical model output and altimeter data. *J. Phys. Oceanogr.*, **27**, 2219–2232, doi:10.1175/1520-0485(1997)027<2219:TSOMBE>2.0.CO;2.

——, M. M. Carranza, R. Cambra, and R. Morrow, 2014: Wind-induced upwelling in the Kerguelen Plateau region. *Biogeosci. Discuss.*, **11**, 8373–8397, doi:10.5194/bgd-11-8373-2014.

Hallberg, R., and A. Gnanadesikan, 2006: The role of eddies in determining the structure and response of the wind-driven Southern Hemisphere overturning: Results from the Modeling Eddies in the Southern Ocean (MESO) project. *J. Phys. Oceanogr.*, **36**, 2232–2252, doi:10.1175/JPO2980.1.

Ivchenko, V. O., K. J. Richards, and D. P. Stevens, 1996: The dynamics of the Antarctic Circumpolar Current. *J. Phys. Oceanogr.*, **26**, 753–774, doi:10.1175/1520-0485(1996)026<0753:TDOTAC>2.0.CO;2.

Jayne, S. R., and J. Marotzke, 2002: The oceanic eddy heat transport. *J. Phys. Oceanogr.*, **32**, 3328–3345, doi:10.1175/1520-0485(2002)032<3328:TOEHT>2.0.CO;2.

Johnson, G. C., and H. L. Bryden, 1989: On the size of the Antarctic Circumpolar Current. *Deep-Sea Res.*, **A36**, 39–53, doi:10.1016/0198-0149(89)90017-4.

Killworth, P. D., and M. M. Nanneh, 1994: Isopycnal momentum budget of the Antarctic Circumpolar Current in the Fine Resolution Antarctic Model. *J. Phys. Oceanogr.*, **24**, 1201–1223, doi:10.1175/1520-0485(1994)024<1201:IMBOTA>2.0.CO;2.

LaCasce, J. H., and P. Isachsen, 2010: The linear models of the ACC. *Prog. Oceanogr.*, **84**, 139–157, doi:10.1016/j.pocean.2009.11.002.

Large, W. G., J. C. Mcwilliams, and S. C. Doney, 1994: Oceanic vertical mixing: A review and a model with a nonlocal boundary layer parameterization. *Rev. Geophys.*, **32**, 363–403, doi:10.1029/94RG01872.

Lee, T., I. Fukumori, D. Menemenlis, Z. Xing, and L. Fu, 2002: Effects of the Indonesian Throughflow on the Pacific and Indian Oceans. *J. Phys. Oceanogr.*, **32**, 1404–1429, doi:10.1175/1520-0485(2002)032<1404:EOTITO>2.0.CO;2.

Levitus, S., and T. P. Boyer, 1994: *Temperature*. Vol. 4, *World Ocean Atlas 1994*, NOAA Atlas NESDIS 4, 117 pp.

Livermore, R., A. Nankivell, G. Eagles, and P. Morris, 2005: Paleogene opening of Drake Passage. *Earth Planet. Sci. Lett.*, **236**, 459–470, doi:10.1016/j.epsl.2005.03.027.

Loveday, B. R., J. V. Durgadoo, C. J. C. Reason, A. Biastoch, and P. Penven, 2014: Decoupling of the Agulhas leakage from the Agulhas Current. *J. Phys. Oceanogr.*, **44**, 1776–1797, doi:10.1175/JPO-D-13-093.1.

Lu, J., and K. Speer, 2010: Topography, jets, and eddy mixing in the Southern Ocean. *J. Mar. Res.*, **68**, 479–502, doi:10.1357/002224010794657227.

MacCready, P., and P. B. Rhines, 2001: Meridional transport across a zonal channel: Topographic localization. *J. Phys. Oceanogr.*, **31**, 1427–1439, doi:10.1175/1520-0485(2001)031<1427:MTAAZC>2.0.CO;2.

Marshall, J., and T. Radko, 2003: Residual-mean solutions for the Antarctic Circumpolar Current and its associated overturning circulation. *J. Phys. Oceanogr.*, **33**, 2341–2354, doi:10.1175/1520-0485(2003)033<2341:RSFTAC>2.0.CO;2.

——, C. Hill, L. Perelman, and A. Adcroft, 1997: Hydrostatic, quasi-hydrostatic, and nonhydrostatic ocean modeling. *J. Geophys. Res.*, **102**, 5733–5752, doi:10.1029/96JC02776.

Masich, J., T. K. Chereskin, and M. R. Mazloff, 2015: Topographic form stress in the Southern Ocean state estimate. *J. Geophys. Res. Oceans*, **120**, 7919–7933, doi:10.1002/2015JC011143.

Meijers, A. J. S., A. Klocker, N. Bindoff, G. Williams, and S. Marsland, 2010: The circulation and water masses of the Antarctic shelf and continental slope between 30 and 80°E. *Deep-Sea Res. II*, **57**, 723–737, doi:10.1016/j.dsr2.2009.04.019.

Munk, W., and E. Palmen, 1951: Note on the dynamics of the Antarctic Circumpolar Current. *Tellus*, **3A**, 53–55, doi:10.1111/j.2153-3490.1951.tb00776.x.

Ohshima, K. I., and Coauthors, 2013: Antarctic Bottom Water production by intense sea-ice formation in the Cape Darnley polynya. *Nat. Geosci.*, **6**, 235–240, doi:10.1038/ngeo1738.

Orsi, A. H., T. Whitworth III, and W. D. Nowlin Jr., 1995: On the meridional extent and fronts of the Antarctic Circumpolar Current. *Deep-Sea Res. I*, **42**, 641–673, doi:10.1016/0967-0637(95)00021-W.

Park, Y.-H., F. Vivier, F. Roquet, and E. Kestenare, 2009: Direct observations of the ACC transport across the Kerguelen Plateau. *Geophys. Res. Lett.*, **36**, L18603, doi:10.1029/2009GL039617.

Redi, M. H., 1982: Oceanic isopycnal mixing by coordinate rotation. *J. Phys. Oceanogr.*, **12**, 1154–1158, doi:10.1175/1520-0485(1982)012<1154:OIMBCR>2.0.CO;2.

Richardson, P. L., 2007: Agulhas leakage into the Atlantic estimated with subsurface floats and surface drifters. *Deep-Sea Res. I*, **54**, 1361–1389, doi:10.1016/j.dsr.2007.04.010.

Rosso, I., A. M. Hogg, P. G. Strutton, A. E. Kiss, R. Matear, A. Klocker, and E. van Sebille, 2014: Vertical transport in the ocean due to sub-mesoscale structures: Impacts in the Kerguelen region. *Ocean Modell.*, **80**, 10–23, doi:10.1016/j.ocemod.2014.05.001.

——, ——, A. E. Kiss, and B. Gayen, 2015: Topographic influence on submesoscale dynamics in the Southern Ocean. *Geophys. Res. Lett.*, **42**, 1139–1147, doi:10.1002/2014GL062720.

Sallée, J., K. Speer, and S. Rintoul, 2011: Mean-flow and topographic control on surface eddy-mixing in the Southern Ocean. *J. Mar. Res.*, **69**, 753–777, doi:10.1357/002224011799849408.

Sparrow, M. D., K. J. Heywood, J. Brown, and D. P. Stevens, 1996: Current structure of the south Indian Ocean. *J. Geophys. Res.*, **101**, 6377–6391, doi:10.1029/95JC03750.

Stevens, D. P., and V. O. Ivchenko, 1997: The zonal momentum balance in an eddy-resolving general-circulation model of the Southern Ocean. *Quart. J. Roy. Meteor. Soc.*, **123**, 929–951, doi:10.1002/qj.49712354008.

Straub, D. N., 1993: On the transport and angular momentum balance of channel models of the Antarctic Circumpolar Current. *J. Phys. Oceanogr.*, **23**, 776–782, doi:10.1175/1520-0485(1993)023<0776:OTTAAM>2.0.CO;2.

Thompson, A. F., and J.-B. Sallée, 2012: Jets and topography: Jet transitions and the impact on transport in the Antarctic Circumpolar Current. *J. Phys. Oceanogr.*, **42**, 956–972, doi:10.1175/JPO-D-11-0135.1.

——, and A. C. Naveira Garabato, 2014: Equilibration of the Antarctic Circumpolar Current by standing meanders. *J. Phys. Oceanogr.*, **44**, 1811–1828, doi:10.1175/JPO-D-13-0163.1.

Toggweiler, J., and B. Samuels, 1995: Effect of Drake Passage on the global thermohaline circulation. *Deep-Sea Res. I*, **42**, 477–500, doi:10.1016/0967-0637(95)00012-U.

Trenberth, K. E., J. G. Olson, and W. G. Large, 1989: A global ocean wind stress climatology based on ECMWF analyses. Climate and Global Dynamics Division, National Center for Atmospheric Research Tech. Note NCAR/TN-388+STR, 98 pp.

van Sebille, E., P. J. van Leeuwen, A. Biastoch, C. Barron, and W. P. M. de Ruijter, 2009: Lagrangian validation of numerical drifter trajectories using drifting buoys: Application to the Agulhas system. *Ocean Modell.*, **29**, 269–276, doi:10.1016/j.ocemod.2009.05.005.

Ward, M., and A. Hogg, 2011: Establishment of momentum balance by form stress in a wind-driven channel. *Ocean Modell.*, **40**, 133–146, doi:10.1016/j.ocemod.2011.08.004.

Waterman, S., A. C. Naveira Garabato, and K. L. Polzin, 2013: Internal waves and turbulence in the Antarctic Circumpolar Current. *J. Phys. Oceanogr.*, **43**, 259–282, doi:10.1175/JPO-D-11-0194.1.

Weijer, W., and Coauthors, 2012: The Southern Ocean and its climate in CCSM4. *J. Climate*, **25**, 2652–2675, doi:10.1175/JCLI-D-11-00302.1.

Williams, R. G., C. Wilson, and C. W. Hughes, 2007: Ocean and atmosphere storm tracks: The role of eddy vorticity forcing. *J. Phys. Oceanogr.*, **37**, 2267–2289, doi:10.1175/JPO3120.1.

Wong, A. P. S., N. L. Bindoff, and A. Forbes, 1998: Ocean-ice shelf interaction and possible bottom water formation in Prydz Bay, Antarctica. *Ocean, Ice, and Atmosphere: Interactions at the Antarctic Continental Margin*, S. S. Jacobs and R. F. Weiss, Eds., Antarctic Research Series, Vol. 75, Amer. Geophys. Union, 173–187, doi:10.1029/AR075p0173.